

# Routes to Ignition on ITER by means of Neutral Beams

H P L de Esch.

JET Joint Undertaking, Abingdon, Oxfordshire, OX14 3EA,

December 1997

"This document is intended for publication in the open literature. It is made available on the understanding that it may not be further circulated and extracts may not be published prior to publication of the original, without the consent of the Publications Officer, JET Joint Undertaking, Abingdon, Oxon, OX14 3EA, UK".

"Enquiries about Copyright and reproduction should be addressed to the Publications Officer, JET Joint Undertaking, Abingdon, Oxon, OX14 3EA".

## 1. INTRODUCTION

The aim of this work is to assess the effect of Neutral Beams on the current version of ITER, principally in terms of the ability to ignite the plasma using Neutral Beam Injection (NBI). Previous work on Neutral Beams for ITER [1] modelled ITER using Rebut-Lallia-Watkins (RLW) transport [2] in L-mode. Because the RLW model is offset-linear, the confinement at high power is at least as good as for conventional H-mode scaling laws, so in effect an H-mode with excellent helium pumping properties was obtained [1]. Little attention to the L→H mode power threshold was paid in that work, as the possibility of a high threshold had just barely started to emerge. Moreover, thanks to the offset-linear properties of the RLW model, plenty of alpha particle power is generated in L-mode, because the confinement gradually improves on L-mode scaling laws like ITER89-P with increasing input power. This *enhanced L-mode confinement* would make it much easier to cross the L→H mode power threshold.

The present work makes use of the JET transport model by Taroni, Cherubini, Erba, Parail and Springmann [3]. A feature of this model is that the transport in the whole of the plasma depends on the edge temperature and edge temperature gradient. The model is implemented in the JET version of the PRETOR code [1,4,5], which is the vehicle for the present simulations.

To model the H-mode, an artificial barrier is introduced to the simulation code when the input power exceeds the H-mode threshold. The width of the barrier is 7.5% of the minor radius. The transport inside this barrier is chosen such, that the global confinement is L-mode or H-mode. Moreover, ELMs are explicitly modelled by switching on the L-mode for a short period of time when the ballooning limit is exceeded over the H-mode transport barrier.

Using this new model, which is different to the models used before, the route to ignition on ITER by NBI is explored. Various beam energies are considered and the plasma rotation resulting from the momentum input of the beams is described.

## 2. ITER 1997 PARAMETERS AND MODELLING.

The ITER parameters and modelling information are taken from the IAEA 1996 (Montreal) conference [6]. Some additional information is obtained from the draft 1997 DDR report (dated 12 November 1996) [7].

The following information was used in the PRETOR runs:

### **Basic plasma:**

$I_p=21$  MA,  $B_T=5.7$  T,  $K=1.7$ ,  $R_0=8.14$  m,  $a=2.8$  m,  $q_{95}=3$ ,  $V=2000$  m<sup>3</sup>,  $S=1200$  m<sup>2</sup>.

A 2% Beryllium impurity has been assumed. Helium is produced by fusion. All species are pumped at the edge, assuming a removal rate of 2% of the particle flux at the edge.

## Neutral Beam Injectors:

Tangency Radius: 6.5 m.

Beam Energy: variable ( 1 MeV is the standard design value (IAEA-96 [8]) )

Beam Power: 0-100 MW ( 50 MW is the standard design value (IAEA-96 [8]) )

The simulations consider plasmas heated by NBI alone. No RF heating is added.

## Thermal confinement times:

L-mode:  $\tau_{96} = 0.023 A^{0.2} I^{0.96} B^{0.03} K^{0.64} R^{1.89} a^{-0.06} n^{0.4} P^{-0.73}$  (IAEA-96 [9], [21])

Elmy H-mode:  $\tau_{93HE} = 0.0306 A^{0.41} I^{1.06} B^{0.32} K^{0.66} R^{1.9} a^{-0.11} n^{0.17} P^{-0.67}$  [9,10]

A is the isotope mass and n is the volume average density in units of  $10^{19} \text{ m}^{-3}$ . This L-mode scaling is also valid in the Ohmic regime, which makes it useful for simulations.

## L→H mode Power threshold:

$$P_{th} = 0.08 n^{0.75} B R^2 \text{ [9]}$$

Simulations have been performed with and without the assumption of a hysteresis for the back transition (H→L mode). The scaling for the L→H mode threshold power is derived from 100% deuterium plasmas. The latest results from JET [15,16] strongly suggest a lower barrier for DT plasmas and simulations with a lower numerical coefficient for the threshold power have been performed as well.

The current expressions for the threshold power are derived by expressing the total input power in terms of n, B and R. However, from the physical point of view, taking the power crossing the separatrix seems more appropriate than taking the input power. This implies that the radiated power in the core plasma has to be taken into account. In present day tokamaks the difference is minimal: The expressions with and without inclusion of the radiated power are the same within the error bars [14].

In ITER the situation will be different as the core plasma will radiate a significant amount of power. If it is indeed the power through the separatrix or the power into the H-mode barrier that matters, the radiated power in ITER will have to be *added* to the current estimates for the threshold power. Simulations with the radiated power added to the input power for the calculation of the threshold power have been performed as well in the present work.

## Local Transport Model:

The heat diffusivity coefficients are prescribed by the JET local transport model [3]. The particle diffusivity coefficients are chosen to be all equal to the electron heat diffusivity coefficient. All

particle pinch velocities are assumed to be equal to the small neoclassical pinch velocities. No anomalous particle pinch velocity has been assumed. As a consequence, all density profiles are quite flat.

### **H-mode edge barrier model**

The H-mode barrier is assumed to have a small heat and particle diffusivity. It is assumed that the barrier has a width of  $7^{1/2}\%$  of the minor radius. The precise diffusivity is determined by feedback on the global confinement time  $\tau_{93}\text{HE}$ . The local transport in the bulk plasma (*inside* the H-mode barrier) remains unchanged.

### **ELM's**

ELM's are explicitly modelled by setting the timestep to 0.1 ms in PRETOR and switching on L-mode. Kukushkin and Pacher *et al.* [11] published an expression for the energy loss per type I ELM. It reads:

$$\Delta W/W = 0.00124 S(\text{m}^2) B(\text{T}) / P(\text{MW})$$

The ELM is switched off in PRETOR when the plasma energy has dropped by at least  $\Delta W$  since the ELM was triggered. The ELM is triggered when the kinetic edge pressure gradient exceeds the ballooning limit in the edge.

### **Ballooning Limit in the core plasma**

When the pressure gradient in the core plasma exceeds the ballooning limit (we adopted the formula from Pogutse-Yurschenko [12]), the transport ( $\chi_i$  and  $\chi_e$ , and  $D$  as a consequence) is locally increased in such a way that the plasma pressure remains at the ballooning limit.

### **Plasma Rotation**

Rotation is modelled by considering the torque given by the beams and by assuming that the radial momentum diffusivity coefficient  $\chi_\phi$  is equal to the ion heat diffusivity coefficient  $\chi_i$ , as observed in JET and TFTR [17,18]. On other tokamaks, it was at least observed that  $\chi_\phi$  and  $\chi_i$  have similar values, see e.g. [19]. Because the plasma rotates, some beam power is not transferred to the plasma. This "lost" power is, however, compensated by the power dissipated by rotation which has a broader profile. These small contributions are taken into account in PRETOR.

## **3. DIFFERENCES BETWEEN OUR MODELLING AND THE ITER TEAM MODELLING.**

We kept to the same modelling as the ITER team (IAEA 1996 Montreal [6,9,11,13] and DDR

draft report [7] for more details), except for the following differences.

- Neutral Beams have been explicitly modelled [1]. The ITER team use ‘*idealised heating*’ which deposits the power in the centre of the plasma and assume that half the power couples to the ions.
- The ITER team have a divertor model and model argon seeding. This is not in our version of PRETOR and not important for assessing the effects of Neutral Beams.
- The ITER team use the RLW model for local transport, we use the JET model (We have previously published our RLW simulations [1]).
- The ITER team do not model the ELM’s explicitly.
- The ITER team adjust the bulk transport in order to get the global confinement time right. We adjust the H-mode edge barrier only to do this job.

When using RLW local transport it is not possible to adjust the edge barrier to match the global confinement time. This is because at high input power RLW gives better confinement than  $\tau_{93}\text{HE}$ . Nothing is left in the edge to adjust!

- The ITER team have recently published (in the DDR draft [7]) simulations where the radiated power is subtracted from the input power for the purpose of the calculation of the L→H threshold power and the confinement time. We have done simulations with and without the inclusion of the radiated power in the calculation of the L→H threshold power.

#### **4. STANDARD SIMULATION.**

Our standard simulation starts with a plasma with plasma current  $I=21$  MA and toroidal field  $B=5.7$  T. The volume average density  $n$  is  $3 \cdot 10^{19} \text{ m}^{-3}$ . At 15 seconds the deuterium beams are switched on and trigger the H-mode if enough power is applied. At 25 seconds the plasma density is increased by puffing 50:50 DT gas in the edge. Flat top density is reached at 77.5 seconds. The beams are ramped down between 100 seconds and 150 seconds. This could be done much earlier in time. The reason for continuing the NBI heating is to obtain the plasma rotation. At 400 seconds the simulation is stopped. We did not try to model plasma shutdown.

#### **5. L-MODE MODELLING RESULTS.**

Figure 1 shows a simulation where no feedback on a global confinement time was done. No H-mode barrier was imposed either. The purpose of this is to demonstrate the performance of the JET model with the chosen coefficients in terms of the ITER89-P scaling law. 100 MW of 1 MeV beams was applied. Figure 1 shows that  $1.2 \cdot \text{ITER89-P}$  is transiently reached before the value drops to  $1.0 \cdot \text{ITER89-P}$  after a sawtooth crash. The alpha power transiently reaches 80 MW, before falling back to 40 MW after a sawtooth. The latter value is also mentioned by the ITER team [9].

The conclusion from this is that the L-mode on ITER is credibly modelled and that we can go to the next stage by imposing an H-mode barrier.

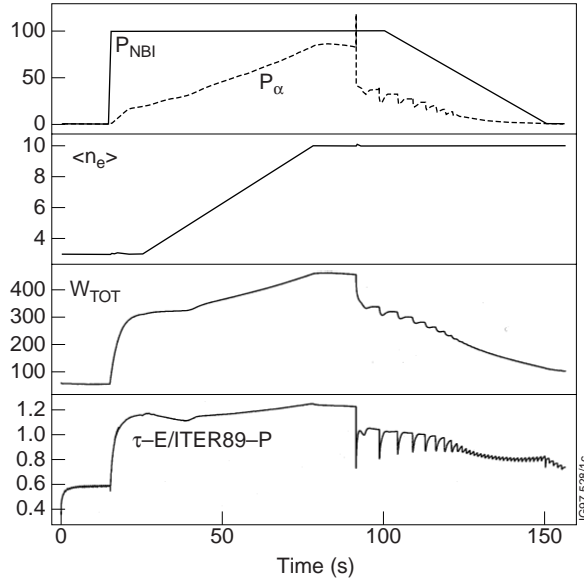


Fig. 1: Simulation of an ITER L-mode discharge, using the JET mixed Bohm-GyroBohm transport model [3]. No feedback on a global confinement time scaling law is applied.

- (a) 1 MeV Beam Power (MW) and the alpha particle power generated.
- (b) Volume Average Density in units of  $10^{19} \text{ m}^{-3}$ .
- (c) Total Stored Energy in MJ.
- (d) Confinement Time relative to the ITER89-P Confinement Time Scaling.

## 6. STANDARD ELMY H-MODE SIMULATIONS

In these simulations 100 MW of 1 MeV beams was applied to a  $3 \cdot 10^{19} \text{ m}^{-3}$  plasma. The density was ramped to various final densities. In figure 2 we give an example where the volume average density was ramped to  $10^{20} \text{ m}^{-3}$ . ITER93-HE energy confinement was maintained by feedback on the transport coefficients in the H-mode barrier. The ELMS are explicitly modelled, which accounts for the dense appearance of the radiated power trace. In the example in figure 2, the helium concentration reaches 8% and the tritium concentration reaches a low point of 42%.

In figure 3, the time slice between 301 and 305 seconds is expanded to show the ELM's. The 4% variation in stored energy due to the ELM's can clearly be seen. Feedback on  $\tau_{03}\text{HE}$  is maintained by switching feedback off during an ELM. The increase in alpha power during an ELM is caused by the decrease in electron temperature during an ELM, which enhances the slowing down of the large population of alpha particles present. The fine structure visible on it is due to the peculiarities of our modelling.

Figure 2 shows that the minimum alpha power for a  $10^{20} \text{ m}^{-3}$  plasma is just above 200 MW. If the threshold for the H→L back transition would be in excess of 200 MW, ignition could not be sustained. Because the alpha power depends more strongly on density than the L→H threshold power, an *ignition domain* can be identified: it gives the lowest density at which

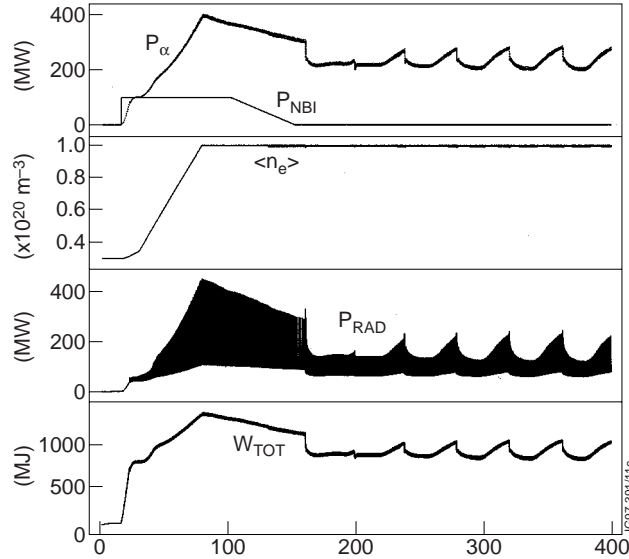


Fig. 2: Example of a Route to Ignition on ITER using 100 MW of 1 MeV NBI and making use of the Elmy H-mode. The H-mode Confinement Time was chosen to be ITER93-HE [9,10]. The L-mode Confinement Time was forced to follow ITER96-L [9].

- 1 MeV Beam Power (MW) and the alpha particle power generated.
- Volume Average Density in units of  $10^{19} \text{ m}^{-3}$ .
- Radiated Power in MW. The black surface in the plot is caused by strong and frequent fluctuations in the radiated power due to ELM's.
- Total Stored Energy in MJ.

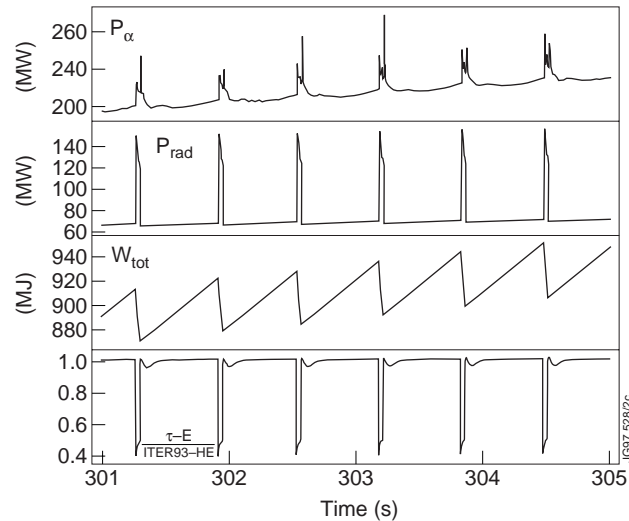


Fig. 3: Expanded view of a simulation of a  $\langle n_e \rangle = 10^{20} \text{ m}^{-3}$  ITER plasma. A time slice between 301 and 305 seconds is shown. An ELM is triggered each time when the ballooning limit across the edge H-mode barrier is exceeded. Shown are:

- The Alpha Particle Power (MW) coupled to ITER.
- The Radiated Power in MW.
- The Stored Energy in MJ.
- The Energy Confinement Time expressed in terms of ITER93-HE [9,10]. The value of appr. 1 in between ELMs is maintained by feedback.



ignition can be sustained for a given L→H threshold power. This lowest density is obviously strongly dependant on the modelling parameters assumed: confinement time scaling, particle transport, helium pumping rate,  $Z_{\text{eff}}$ , transport model, etc. However, it is instructive to make the plot for the current modelling, see figure 4.

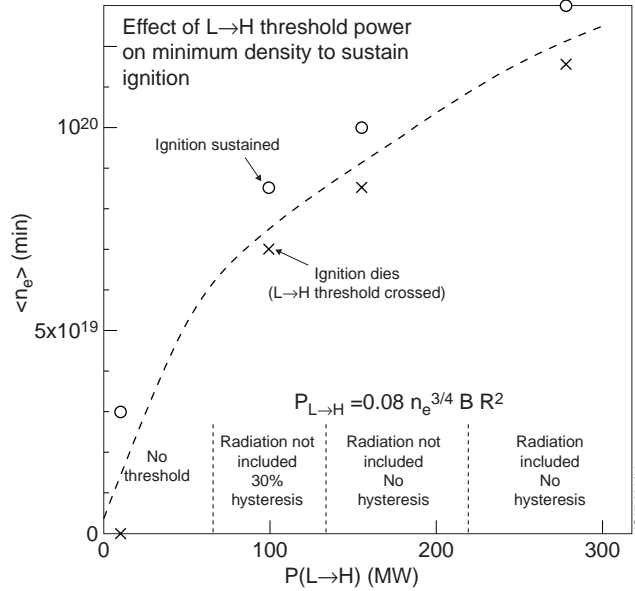


Fig. 4: ITER Ignition Domain: Minimum Density needed to sustain ignition vs. L→H Power Threshold. This plot is valid for the modelling assumptions in section 2. Indicated on the horizontal axis are some physics assumptions on the L→H Power Threshold. Assuming that  $P_{L \rightarrow H} = 0.08 n_e^{3/4} B R^2$ , one can identify:

- If there is no threshold, very low density plasmas can remain ignited.
- If radiation is not added to the threshold power requirement and a 30% hysteresis for the back transition is assumed, a minimum density of around  $8 \cdot 10^{19} \text{ m}^{-3}$  is required. A similar value will be found if no hysteresis is assumed, but a generally lower threshold value  $P_{L \rightarrow H} = 0.055 n_e^{3/4} B R^2$  is assumed due to D-T plasmas.
- If there is no benefit from a hysteresis in the H→L back transition, the minimum density increases to around  $10^{20} \text{ m}^{-3}$ .
- If finally radiation is added to the threshold power requirement and no hysteresis is assumed, a density of  $1.2 \cdot 10^{20} \text{ m}^{-3}$  is required to sustain ignition.

Figure 4 gives the lowest density necessary to sustain ignition for a given L→H threshold power. The recommended scaling for the L→H threshold power is:

$$P_{\text{th}} = 0.08 n^{0.75} B R^2 \quad [9]$$

If no L→H threshold is assumed, ITER93-HE confinement time scaling will keep ITER ignited for almost any density. As soon as a threshold is introduced, the ignition domain shrinks because the plasma must generate sufficient power to overcome the threshold. If one does not subtract radiation from the power that sustains the H-mode ITER operation at  $10^{20} \text{ m}^{-3}$  looks just feasible. If the power into the H-mode barrier is considered to determine whether the plasma is in H or L-mode (ie: radiation is thus subtracted), ignited ITER operation at  $10^{20} \text{ m}^{-3}$  looks unlikely.

Although we did some simulations assuming a hysteresis in the H→L back transition (assuming that once the plasma is in H-mode, less power is needed to sustain the H-mode), recent evidence from JET [14] shows that there is no hysteresis:  $P_{H\rightarrow L} = P_{L\rightarrow H}$ . On a more positive note: further recent evidence from JET [15,16] shows that the L→H threshold power is significantly reduced (scaling like  $1/A$ ) when operating in DT rather than pure deuterium.

We have included figures in which we show the profiles taken at 99 seconds into the simulation. At this point in time the density has reached its flat top, but the 100 MW of 1 MeV beams is still on. The first sawtooth hasn't occurred yet. The discharge is very elmy, but the datapoints themselves are taken in between ELM's. Profiles are given for volume average densities between 7 and  $14.5 \cdot 10^{19} \text{ m}^{-3}$ .

In figure 5, the electron density, electron temperature, ion temperature and total pressure ( $p=n_e kT_e+n_i kT_i$ ) profiles are plotted for the six different plasma densities.

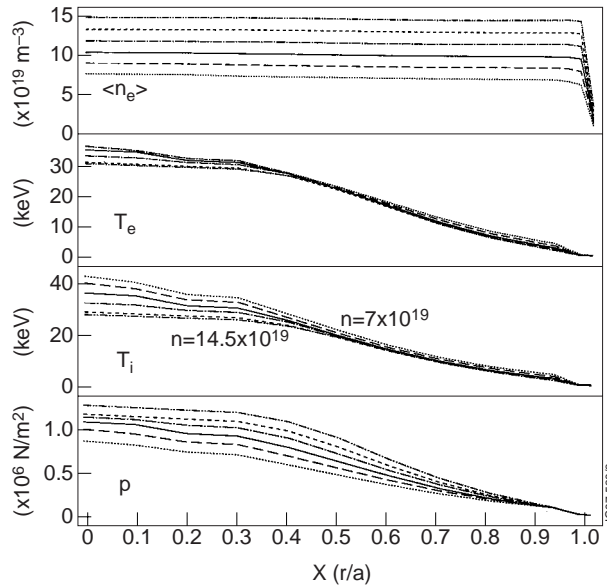


Fig. 5: Simulated Elmy H-mode Profiles at  $t=99\text{s}$  in a standard simulation. 100 MW of 1 MeV Beams into plasmas with densities in the range of  $7\text{-}14.5 \cdot 10^{19} \text{ m}^{-3}$ .

- (a) Density Profiles in  $10^{19} \text{ m}^{-3}$ .
- (b) Electron Temperature Profiles in keV.
- (c) Ion Temperature Profiles in keV.
- (d) Pressure ( $p=n_e kT_e+n_i kT_i$ ) Profiles in  $\text{N/m}^2$ .

In figure 6, the heat diffusivities  $\chi_e$  and  $\chi_i$  are shown. The peak at  $r/a=0.2$  is caused by the ballooning limit in the bulk plasma. The depression between  $r/a=0.9$  and  $1.0$  is the H-mode barrier. Whereas in the JET transport model  $\chi_e$  and  $\chi_i$  are different, they are always chosen the same in the H-mode transport barrier. The value of the barrier is determined by the requirement of maintaining a global confinement time  $\tau_{93}\text{HE}$ .

In figure 7 profiles of the NBI fast particle source rate (in  $10^{18} \text{ m}^{-3} \text{ s}^{-1}$ ), the total NBI power (in  $\text{MW/m}^3$ ) and the NBI fast particle density (in  $10^{19}$  beam ions per cubic metre) are shown.

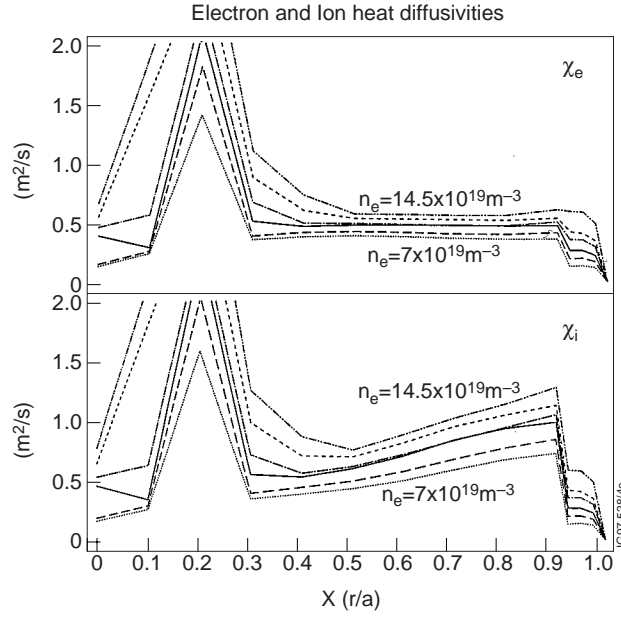


Fig. 6: Simulated Elmy H-mode Profiles at  $t=99s$  in a standard simulation. 100 MW of 1 MeV Beams into plasmas with densities in the range of  $7\text{-}14.5 \cdot 10^{19} \text{ m}^{-3}$ .

- (a) Electron Heat Diffusivity Profiles in  $\text{m}^2/\text{s}$ .
- (b) Ion Heat Diffusivity Profiles in  $\text{m}^2/\text{s}$ .

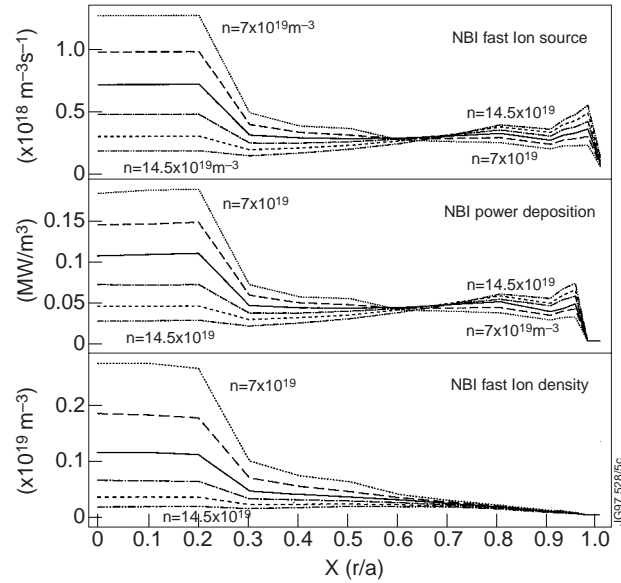


Fig. 7: Simulated Elmy H-mode Profiles at  $t=99s$  in a standard simulation. 100 MW of 1 MeV Beams into plasmas with densities in the range of  $7\text{-}14.5 \cdot 10^{19} \text{ m}^{-3}$ .

- (a) NBI Fast Ion Source Rate Profiles in  $10^{18} \text{ m}^{-3} \text{ s}^{-1}$ .
- (b) NBI Power Deposition Profiles in  $\text{MW}/\text{m}^3$ .
- (c) NBI Fast Particle Density Profiles in  $10^{19} \text{ m}^{-3}$ .

In figure 8 the fraction of NBI power (in %) coupled to the ions is shown. This power fraction to the ions is remarkably constant for the various plasma densities. The reason for this is that the electron temperature also hardly changes (figure 5). The reason for the nearly constant electron temperature is the increasing fusion power with density.

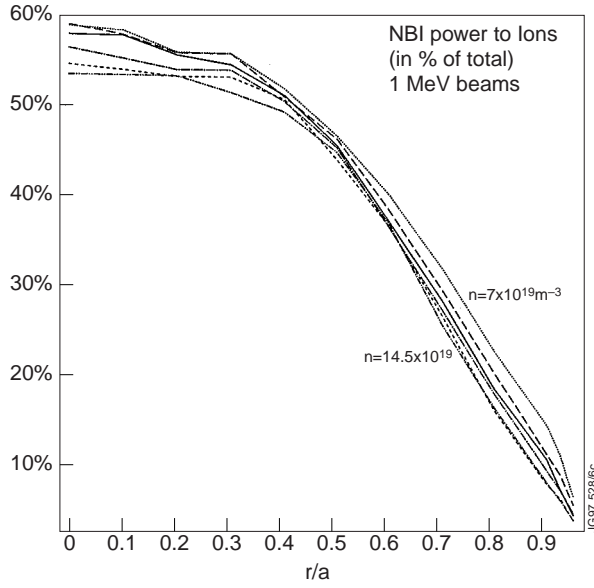


Fig. 8: Fraction of NBI Power coupled to the Ions in Elmy H-mode ITER Plasmas. 100 MW of 1 MeV Beams into plasmas with densities in the range of  $7\text{-}14.5 \cdot 10^{19} \text{ m}^{-3}$ .

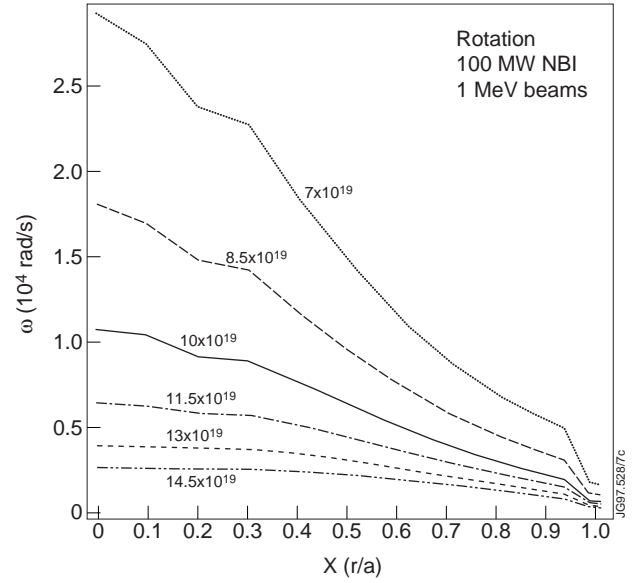


Fig. 9: Simulated ITER Rotation Profiles as a result of 100 MW of 1 MeV Beams injected into ELMy H-mode plasmas with densities in the range of  $7\text{-}14.5 \cdot 10^{19} \text{ m}^{-3}$ . The angular velocities are expressed in units of  $10^4 \text{ rad/s}$ .

In figure 9 the plasma rotation (in  $10^4 \text{ rad/s}$ ) profiles are shown.

## 7. MINIMUM POWER TO IGNITE ITER

The minimum power to ignite ITER is determined by the power needed to achieve an H-mode. The alpha power generated in L-mode, helps only marginally (if only because the density is low in order to keep the H-mode threshold low!). Once the H-mode is achieved almost no additional power is needed to ignite the plasma because of the good H-mode confinement. Keeping the density low is beneficial for crossing the threshold. However, below a certain optimum density, the threshold power increases again with lower density. This is possibly due to an increase in neutral particles in the edge plasma at very low density [20].

In our simulations we started all plasmas at  $n=3 \cdot 10^{19} \text{ m}^{-3}$ . We did not attempt to ramp plasma current or toroidal field. Neither have the ITER team published such simulations. Therefore,  $P_{\text{th}}$  is determined at  $n=3 \cdot 10^{19} \text{ m}^{-3}$  and  $B=5.7 \text{ T}$ . This gives  $P_{\text{th}}=69 \text{ MW}$ .

Once the H-mode is triggered, the density is ramped up to  $10^{20} \text{ m}^{-3}$  and ignition is achieved. Very little additional power is needed for ignition once the H-mode is triggered. Ignition might be lost later in time, if the alpha power is lower than the power to maintain the H-mode. This can happen after a sawtooth, once helium has accumulated in the plasma.

The minimum NBI power to ignite ITER was determined by running a number of simulations and finding the power below which no ignition could be achieved. This was invariably the NBI power needed to trigger the H-mode with assistance from the alpha particle power

including the beam-plasma alpha particle power. We performed simulations for 5 different beam energies, ranging from 125 keV to 1 MeV. For each case we performed simulations assuming the standard L→H threshold power ( $P_{th} = 0.08 n^{0.75} B R^2$ ) and a more optimistic version ( $P_{th} = 0.055 n^{0.75} B R^2$ ) in line with the latest JET DT results [15]. Moreover, for each of these 10 cases we ran the case with radiated power added to the threshold power and radiated power omitted.

The resulting 20 cases are plotted in figure 10. Added to the graph are 5 cases of simulations using RLW transport from ref. [1]. It can be seen that the beam energy makes little difference to the minimum power required to ignite ITER. Basically, all power that is deposited inside the separatrix is “counted in”. Major differences in the power requirement are caused by the physics assumptions. The key assumptions relate to the L→H threshold power and the question whether the power flowing out past the separatrix, rather than the power coupled to the plasma is to be taken for the L→H threshold power.

Having established that the minimum power to ignite ITER mainly depends on assumptions related to the H-mode threshold, we can take a look at some details in the following subsections.

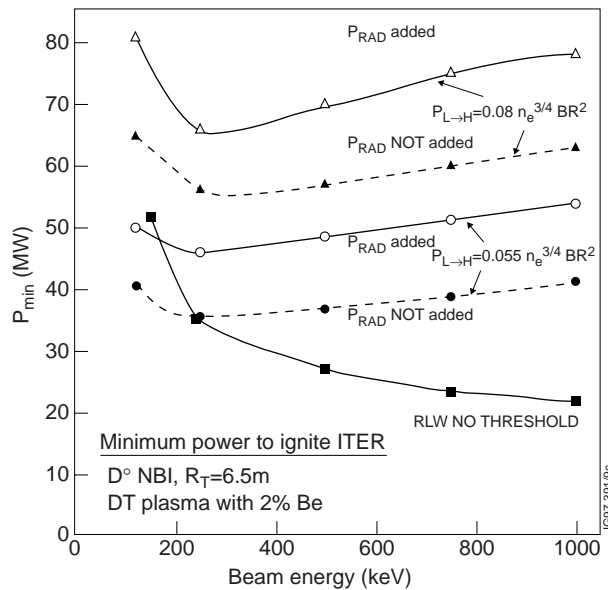


Fig. 10: Minimum NBI Power to ignite ITER. This minimum power requirement is calculated for 5 different beam energies and appears to depend mainly on the physics assumptions:

- (a) bottom curve: RLW transport with no feedback on global confinement time from ref. [1]. No L→H mode threshold was assumed in ref. [1].
- (b) Bottom dashed curve: Assuming an L→H mode threshold, which takes account of JET’s recent favourable results in DT. No radiated power added to the power threshold requirement
- (c) Middle solid curve: As (b), now with radiated power added to the power threshold requirement.
- (d) Top dashed curve: Assuming a pessimistic L→H mode threshold, which does not take account of JET’s recent favourable results in DT. No radiated power added to the power threshold requirement.
- (e) Top curve: The most pessimistic assumption, adding radiated power to the power threshold requirement from (d).

## 7.1 Low Energy NBI

Low energy NBI (down to 250 keV) appears to make crossing the L→H threshold slightly easier. This is because the low-energy NBI generates more alpha particle power in a low density plasma ( $n_e=3 \cdot 10^{19} \text{ m}^{-3}$ ). The extra alpha power is generated due to more central beam deposition, more beam power to the ions and more beam-plasma power (see figure 11). These benefits fall off sharply below 250 keV. The RLW case from [1] is more sensitive to beam energy (figure 10) because in the absence of an H-mode barrier to keep the power in, the poorer penetration of the beams at higher density does matter.

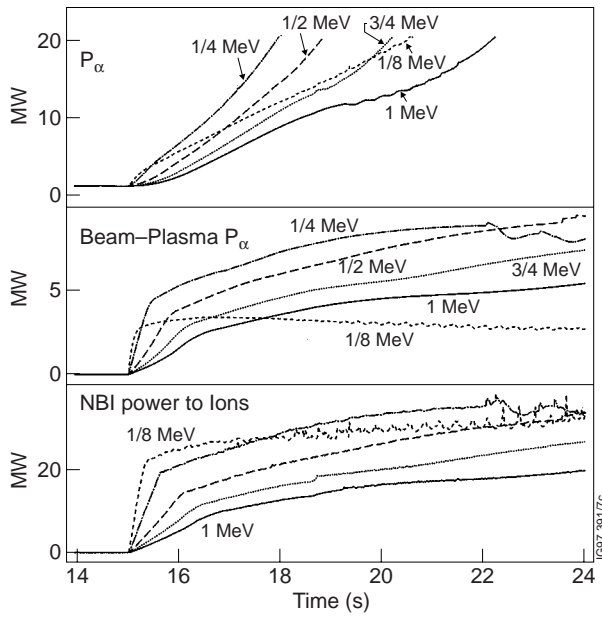


Fig. 11: Onset of crossing the L→H mode threshold in a  $n_e=3 \cdot 10^{19} \text{ m}^{-3}$  plasma. 60 MW NBI is applied at beam energies of 1000, 750, 500, 250 and 125 keV.  $P_{L \rightarrow H} = 0.08 n_e^{3/4} B R^2$  with no radiation added, corresponding to curve d) in fig. 10.

- (a) Alpha Particle Power coupled to the Plasma.
- (b) Beam-Plasma contribution to the Alpha Particle Power.
- (c) Total NBI Power coupled to the Ions.

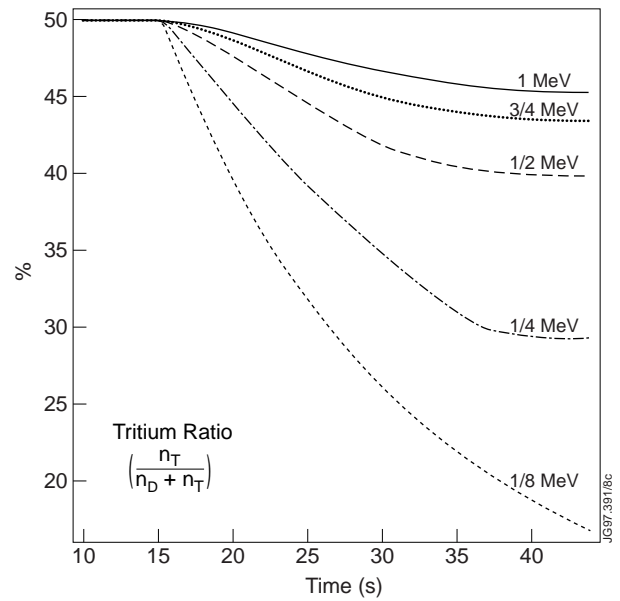


Fig. 12: Development of the tritium content of the plasma before ignition for deuterium NBI at various values for the beam energy.

Figure 12 shows that significant fuel dilution problems begin to occur at  $E_{\text{beam}} < 250 \text{ keV}$ . This raises again the minimum power to ignite ITER. The 125 kV NBI case actually failed to ignite due to fuel dilution problems. In order to achieve ignition with 125 keV  $D^0$  beams, the tritium ratio in the plasma gas had to be raised to 70%.

## 7.2 Power Deposition Profiles

Figure 13 gives the beam power deposition profiles to the ions for 60 MW beams into a  $3 \cdot 10^{19} \text{ m}^{-3}$  plasma. The beam energies are 1 MeV, 500 keV, 250 keV and 125 keV. Also the alpha particle power density profiles (to ions and electrons) are plotted in figure 13.

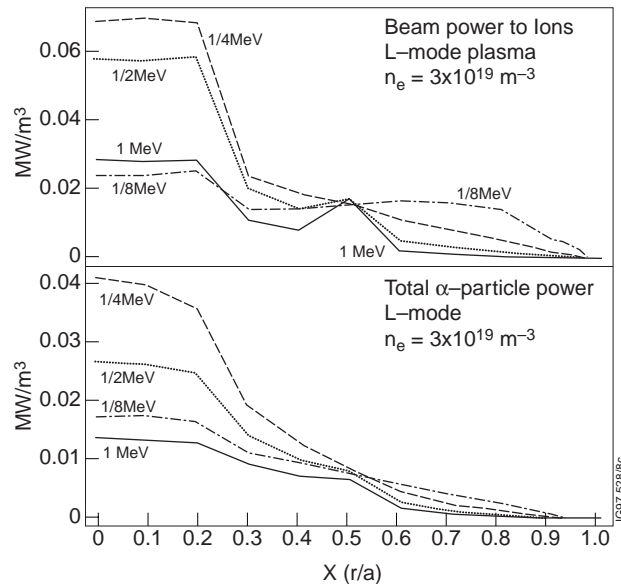


Fig. 13: Simulated L-mode Profiles at  $t=17s$  in a standard simulation. 60 MW of Beams into a  $n_e=3 \cdot 10^{19} \text{ m}^{-3}$  plasma. Beam Energies are 1000, 500, 250 and 125 keV.

- (a) NBI Powerdensity Coupled to the ions in  $\text{MW/m}^3$ .  
 (a) Total Alpha Particle Powerdensity in  $\text{MW/m}^3$ .

## 7.3 Plasma Rotation

Rotation profiles are plotted in figures 14 and 15. Figure 14 gives the rotation profiles for different beam energies while the plasma density is still ramping up. The profiles have been taken at  $n_e=6.5 \cdot 10^{19} \text{ m}^{-3}$ . It appears that the central rotation is not very sensitive to beam energy. The rotation at the  $q=2$  surface (located near  $r/a=0.8$ ) varies strongly with beam energy down to very low energies (125 keV). Figure 15 gives the rotation profiles for different beam energies at  $n_e=10^{20} \text{ m}^{-3}$ . Due to the lack of penetration, low energy beams give a lower central rotation. Rotation at  $q=2$ , however, still benefits from reducing the beam energy down to 250 keV.

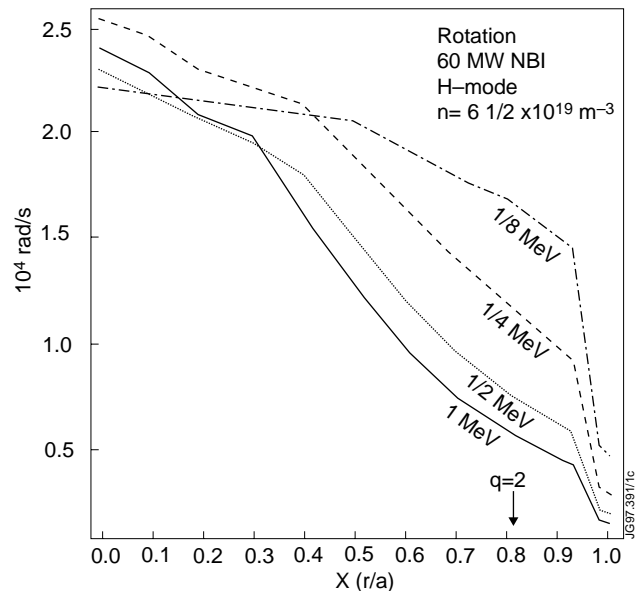


Fig. 14: Simulated Rotation Profiles during the density ramp in ELMy H-mode. 60 MW of Beams into a  $n_e=6.5 \cdot 10^{19} \text{ m}^{-3}$  plasma. Beam Energies are 1000, 500, 250 and 125 keV.

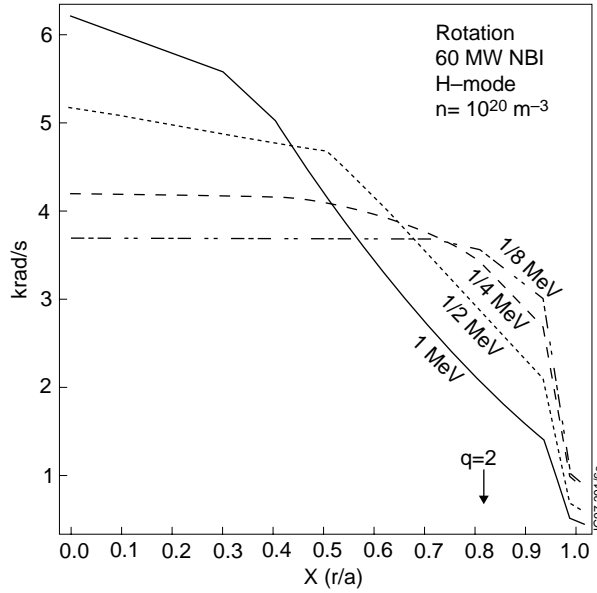


Fig. 15: Simulated Rotation Profiles during the flat top density in ELMy H-mode. 60 MW of Beams into a  $n_e=10^{20} \text{ m}^{-3}$  plasma. Beam Energies are 1000, 500, 250 and 125 keV.

## 8. MIXED ENERGY NBI SCENARIOS

A scheme is conceivable whereby NBI power is provided at low energy (say 125 kV deuterium and/or 190 kV tritium) using existing positive ion technology for the purpose of triggering the H-mode and providing plasma rotation. In addition a source of high energy NBI would provide central heating and current drive.

In figure 16, a simulation is given in which 50 MW of 125 kV deuterium beams (beam fractions 70%, 20% and 10%) were provided for 8 seconds only. 30 MW, 1 MeV beams provide central heating for over 85 seconds. This scheme ignites without problems: the short burst of high power puts the plasma in H-mode, while the low power, high energy NBI sustains the alpha power until the density is high.

Caution should be exercised when considering such low energy scenarios as the effect of the heating profile on the L→H mode

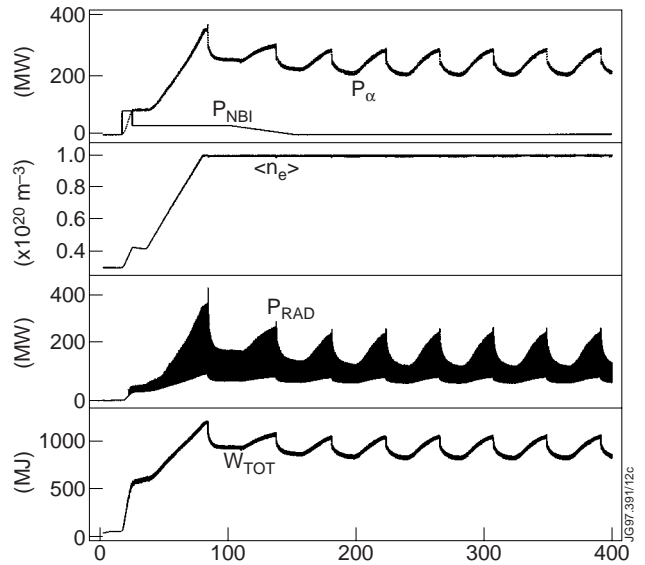


Fig. 16: Simulated ignition achieved by a mixed energy NBI scheme. 50 MW 125 keV NBI was injected for 8 seconds only. 30 MW 1 MeV NBI started simultaneously, but lasted for 85 seconds. The 80 MW of mixed NBI puts the plasma into H-mode, whereas the 30 MW high energy NBI is sufficient to maintain the H-mode together with the Alpha power generated. Ignition is subsequently achieved at higher density.



threshold power is not well established in the database. It is, for example, not established how much of the density dependence of  $P_{L \rightarrow H}$  is a hidden profile effect. As NBI results dominate the database, density and power deposition profile are correlated.

## 9. CONCLUSIONS

Neutral Beams provide an excellent means of bringing the ITER plasma to ignition. The minimum power to ignite ITER does not vary much with beam energy and is dominated by the L→H mode threshold power.

We personally consider the most realistic simulation to be that which uses the JET results for the L→H mode threshold in DT operation [15,16] and *adds* the power radiated within the separatrix to this threshold. On this basis the curve with the open circles in fig. 10 shows that about 50 MW of NBI power is needed to ignite ITER. This figure is largely independent of beam energy but has a shallow minimum at 300 keV for  $D^0$  beams.

For inducing rotation a low energy beam system is best.

At the lowest beam energy studied (125 keV), dilution by the  $D^0$  beams becomes a problem and 250-500 keV seems a sensible compromise.

If very low injection energies are considered for ITER, Neutral Beam Injection in the periphery of the plasma should be studied on present day machines, especially the effect on the L→H transition threshold.

Some interesting mixed energy scenarios can be envisaged.

## ACKNOWLEDGEMENT

The helpful discussions with Dr. D. Stork from JET are highly appreciated.

## REFERENCES

1. H.P.L. de Esch, D. Stork, C. Challis and B. Tubbing, *The optimisation of neutral beams for ignition and burn control on next-step reactors*. Fusion Engineering and Design **26**(1995)589.
2. P-H. Rebut, P.P. Lallia and M.L. Watkins, *The Critical Temperature Gradient Model of Plasma Transport: Applications to JET and Future Tokamaks*. Proc. 12<sup>th</sup> IAEA Int. Conf., Nice, France, 1988, Vol. 2, IAEA, Vienna (1989) 2209.
3. V. Parail, A. Cherubini, M. Erba, E. Springmann and A. Taroni, *Numerical Simulation of ELM Free H- and Hot Ion H-modes JET Plasmas*, JET-P(95)49  
M Erba, A Cherubini, V V Parail, E Springmann and A Taroni, *Development of a non-local model for tokamak heat transport in L-mode, H-mode and transient regimes*, Pl. Phys. Contr. Fusion **39**(1997)261.

4. H.P.L. de Esch, A. Cherubini, J.G. Cordey, M. Erba, T.T.C. Jones, V.V. Parail, D. Stork and A. Taroni, *Simulations of JET Hot-Ion H-modes with a Predictive Code*, Proc. 23<sup>rd</sup> EPS conf. on Contr. Fus. and Pl. Physics, Kiev, Ukraine, 1996, vol 20C(I) p 151.
5. D. Boucher and P.H. Rebut, *Predictive Modelling and Simulation of Energy and Particle Transport in JET*, IAEA technical Committee Meeting, Montréal, Canada, 15-17 June 1992.
6. R. Aymar *et al.*, *ITER Project: A Physics and Technology Experiment*. Proc. 16<sup>th</sup> IAEA Fusion Energy Conference, Montréal, Canada, 1996, paper IAEA-CN-64/01-1.
7. DDR-ITER chapter III, *ITER Physics Basis and Plasma Performance Assessment*, Draft version from 12 November 1996.
8. R. Hemsworth *et al.*, *ITER Neutral Beam Injector Design*. Proc. 16<sup>th</sup> IAEA Fusion Energy Conference, Montréal, Canada, 1996, paper IAEA-CN-64/FP-18.
9. T. Takizuka *et al.*, *Threshold Power and Confinement for ITER*. Proc. 16<sup>th</sup> IAEA Fusion Energy Conference, Montréal, Canada, 1996, paper IAEA-CN-64/F-5.
10. K. Thomsen *et al.*, *ITER H Mode Confinement Database Update*, Nucl. Fusion **34**(1994)131
11. A. Kukushkin, H.D. Pacher *et al.*, *Analysis of the Performance of the ITER Divertor and analysis of the ITER Tokamak Edge Parameter Database*, Proc. 16<sup>th</sup> IAEA Fusion Energy Conference, Montréal, Canada, 1996, paper IAEA-CN-64/FP-27.
12. O.P. Pogutse and E.I. Yurschenko, *Ballooning Effects and Plasma Stability in Tokamaks*, Reviews of Plasma Physics, vol. 11, p65.  
Edited by M.A. Leontovich, Consultants Bureau, Plenum Press, New York.
13. S. Putvinski *et al.*, *ITER Physics*, Proc. 16<sup>th</sup> IAEA Fusion Energy Conference, Montréal, Canada, 1996, paper IAEA-CN-64/F-1.
14. E. Righi *et al.*, *Dedicated ITER H-mode Power Threshold Experiments with the Mki Pumped Divertor*, JET-P(97)28, to be published in Pl. Phys. and Contr. Fusion.
15. J. Jacquinot *et al.*, *ITER Physics Experiments in JET D/T Plasmas*, Proc. 24<sup>th</sup> EPS Conference (Berchtesgaden, Germany), to appear. *Also*: JET-P(97)16, page 137.
16. E. Righi *et al.*, *IAEA Technical Committee Meeting on H-mode Physics (September 1997)*, to be published in Pl. Phys. and Contr. Fusion.
17. H.P.L. de Esch, D. Stork and H. Weisen, *Toroidal Plasma Rotation in JET*. Proc. 17<sup>th</sup> EPS Conf. on Contr. Fusion and Plasma Heating, Amsterdam 1990, Vol 1, p90.
18. S.D. Scott *et al.*, *Correlations of heat and momentum transport in the TFTR tokamak*, Phys. Fluids **B2**(6)1990.
19. O. Gruber, A. Kallenbach, H.-U. Fahrbach, H. Hermann and O. Vollmer, *Ion and Toroidal Momentum Transport with Flat (Co-NBI) and Peaked (Ctr-NBI) Density Profiles in ASDEX*, 16<sup>th</sup> EPS Conf. on Contr. Fusion and Plasma Heating, Venice 1989, Vol I, p171.

20. T. Fukuda *et al.*, *H Mode Transition Threshold Power Scaling and its relation to the Edge Neutrals in JT-60U*. Nuclear Fusion **37**(1997)1199.
21. S.M. Kaye and ITER Confinement Database Working Group, *ITER L Mode Confinement Database*. Nuclear Fusion **37**(1997)1303.